

# **Analysis of the performance of a building solar thermal facade (BSTF) for domestic hot water production.**

A. Gagliano\*, S. Aneli  
Department of Electric, Electronics and Computer Engineering  
University of Catania, Catania, Italy  
e-mail: [antonio.gagliano@dieei.unict.it](mailto:antonio.gagliano@dieei.unict.it)

F. Nocera  
Department of Civil Engineering and Architectural  
University of Catania, Catania, Italy  
e-mail: [fnocera@unict.it](mailto:fnocera@unict.it)

## **ABSTRACT**

New EU ambitious targets of 32% from renewables by 2030 make more and more necessary to satisfy the energy needs of buildings through renewable energy sources.

Thus, the installation of solar collectors applied or integrated into the building envelope may represent an interesting opportunity to increase the fraction of the building energy demands supplied through solar energy.

In particular, the implementation of building solar thermal facades (BSTFs) could be very useful in high-rise buildings, which do not have sufficient spaces where to install a solar plant.

This paper presents the simulations carried out with TRNSYS software to evaluate the energy performances of building solar thermal facades (BSTFs) constructed with two distinct types of solar collectors, flat plate (FPC) and evacuated solar collectors (ETC).

Transient simulations of the two configurations of BSTF were replicated under the climate conditions of four Italian cities: Ragusa, Catania, Rome, and Milan.

The research also provides the results of an economic and LCA analysis, which allow evidencing the different performances between the two types of examined BSTFs.

Moreover, this study presents a preliminary investigation on a prototype of ventilated building solar thermal facade (v-BSTF) built in Ragusa, which is used for Domestic Hot Water (DHW) scope.

The results of simulations highlight that a BSTF facing south, constituted by 4.0 m<sup>2</sup> of FPC, permits to satisfy about 65% of the energy requirements for DHW of a single residential unit, in Ragusa, Catania, and Rome, and of about 44% in Milan. If the BSTF is constructed using ETC, these percentages increase to 57% in Milan and 77% in the other investigated cities.

The high fraction of the DHW energy requirements supplied through a BSTF, as well as the short energy and CO<sub>2</sub> payback times, allows affirming that a south oriented vertical solar façade represents a suitable system for DHW production with great environmental conveniences.

## **KEYWORDS**

Building Solar Thermal Facade, DHW energy needs, thermal performance, TRNSYS simulations, energy and environmental analysis

## 1.0 INTRODUCTION

The diffusion of solar thermal systems for satisfying the energy demand for domestic hot water as well for space heating should be boosted in view to reach the new EU ambitious targets of 32% from renewables by 2030.

The provisional deal provides a sub-target of an indicative 1,3% yearly increase of renewables in heating and cooling installations, calculated on a period of 5 years starting from 2021 [1]

In this context, solar energy represents a decisive issue in renewable energy production that could satisfy the building's energy needs completely or in part. [2]

This means that the integration of active solar systems (photovoltaics, solar thermal and hybrid systems) will be crucial in the design and operation of buildings and their energy systems [3]

Architectural integration is a major issue in the growth and diffusion of solar thermal technologies.

In this way, S. Kalogirou,[4] gave a survey of possible solutions of PV and STS integration on the building roofs and façades. Architectural integration is an important issue in the growth and diffusion of solar thermal technologies. Indeed, Chr. Lamnatou et al. [5], revealed that the majority of the models is about BIPV and skin façades while there are very few studies on BIST systems. Thereby, more investigations on energetic, thermal, optical simulations for BIST installations particularly for active systems (e.g. active solar thermal collectors) are necessary

Building integration of solar collector technology has to be foreseen during the early design stage to replace conventional cladding solutions. Fully integrated façade or roof systems provide the same protective features as conventional building skins (thermal insulation and moisture, wind, and water protection) while generating significant renewable energy throughout their service life as part of the building. Moreover, Buonomano et al. [6] analysed the energy and economic performance of roof and/or façades Building Integrated flat-plate PhotoVoltaic and Thermal (BIPVT) collectors for residential applications. They have developed a simulation model for several case studies representative of a multi-story residential building in different European climates. It has been found out that the adoption of BIPVT panels produces a decrease of the primary energy demands from 67% to 89%, depending on the weather and the building-plant configuration.

The market for Building Integrated Solar Thermal (BIST) collectors is increasing, mainly in countries such as Germany and Austria, where proper incentives have advanced the development of energy-generating building envelopes [7]

The International Energy Agency, Solar Heating and Cooling Programme has supported the task Solar Energy and Architecture (IEA SHC Task 41), which led to providing design criteria and guidelines for achieving high-quality architecture for buildings integrating solar energy systems [8].

F. Motte et al [9] affirmed that the aesthetic of solar thermal collectors can be an obstacle to their development and limits the growth of the market. Consequently, they presented a new-patented concept of flat plate solar collector totally integrated into a gutter. The new complete solar collector consists of several short modules connected serially-

Maurer et al. [10] presented a general methodology to evaluate the economic benefits of building integrated solar thermal systems. They demonstrated that any thermal energy offset by the BISTs generates a saving that can reduce the building's operational cost. Moreover, the BIST system can reduce the overall construction material costs and may offer additional revenue in the form of financial incentives and tax credits.

A detailed study of a BIST thermal performance have been addressed

More in detail, Albanese et al.[11] evaluated performance for an experimental passive solar space heating system utilizing heat pipes to transfer heat through an insulated wall from an absorber outside the building to a storage tank inside the building. The heat pipe system

provided significantly higher solar fractions than the other passive options in all climates but was particularly advantageous in cold and cloudy climates. Buonomano et al. [12] analysed the energy performance of a low-cost water solar collector prototype, designed for the integration into building façade. It has been found out that the use of building integrated solar thermal collectors influences the HVAC energy demand and the indoor hygrothermal comfort in a passive way.

Beccali et al.[13] proposed an analysis of south-façade integrated solar air collectors for a typical Italian building. They performed transient simulations for two different sites in Italy characterized by opposite climatic conditions (Milan and Palermo) in which they showed that the BIST positively affects the yearly energy balance particularly for climates where the heating demand is prevalent.

Other research focused on Finite Element Models (FEM) or Transient System Simulation (TRNSYS) model calculation of integrated component overall performance.

Specifically, Hassan et al.[14] presented a new design for BIST, based upon thermal performance, functional integration, composite behavior, environmental design, durability, sustainability, reliability, flexibility, ease, and speed of construction, and cost-effectiveness.

Antoniadis et al [15], proposed a study on the optimization of a building integrated solar thermal system with seasonal storage using TRNSYS. Two distinct type of solar collectors and two different building integration options were investigated: a roof integrated flat plate solar array and a vacuum tube solar array either integrated into the façade.

Many studies are focused on the thermal performances of Solar Domestic Hot Water System (SDHW). Such topic is worth of relevance considering that in new housing the hot water production reaches sometimes 30% of overall energy consumption, satisfying such energy needs through solar thermal system became a primary objective for reaching the NZEB target.

Notton et al. [16] stated that in the Mediterranean area, a solar thermal plant can satisfy up to 80% of the hot water energy demands with minimal operational and management expense.

Motte et al.[17] estimated the effect of adding a PCM into a building-integrated solar thermal collector in view to improve the thermal performances of an SDHW system.

Gagliano et al. [18] monitored and investigated the performances of a pilot PVT plant for DHW production. Other studies investigated the economic viability of solar systems in both residential [4] and non-residential buildings. The use of flat-plate collectors integrated into the facades of a high-rise residential building in Hong Kong was analysed by Chow et al.[19]

Buonomano et al. [20] developed a new simulation model for the dynamic energy performance analysis of multi-zone buildings of a non-residential NZEB with Building Integrated PhotoVoltaic (BIPV) and PhotoVoltaic/Thermal (BIPV/T) device.

Life-cycle impact assessment (LCA) studies have been also developed for both building added (BAST) and BIST system. S. Kalogirou [21] investigated the environmental benefits of utilising solar energy instead of conventional sources of energy, the different emissions resulting from the solar system operation are estimated and compared to those of a conventional fuel system.

The energy and the life cycle assessment (LCA) of a solar thermal collector for sanitary warm water demand has been investigated following the international standards of series ISO 14040 by Ardente et al. who demonstrated the great energy convenience of such technology [22].

Starting from the results of previous research [22], Ardente et al. investigated an energy balance between the employed energy during the collector life cycle and the energy saved thanks to the collector use. They estimated that, even in pessimistic scenarios, the energy and emission payback times are lower than 4 years [23].

Life-cycle impact assessment studies (LCA) have been also developed for both building added (BAST) and BIST system.

The life-cycle impact assessment methodologies adopted are mainly based on embodied energy and embodied carbon emissions [24].

The aim of this study is to evaluate the viability of façade solar collectors used for DHW production in different climate contexts. Thus, the energy and environmental analysis of evacuated tube solar thermal collectors (ETC) and flat plate solar-thermal collectors are compared and analyzed by means of the software TRNSYS.

Considering that there is a lack of literature studies that investigate the overall performances of such typologies of solar systems, it is worth of interest to evaluate the variation of the energy performances of vertical BSTFs in different climate conditions. The research also provides the results of an LCA and economic analysis, which allow evidencing the different performances between the two types of examined BSTFs.

Moreover, some preliminary results of a survey carried out on the prototype of a ventilated solar facade added to the building envelope (v-BSTF) developed within the research project “Solar Collector Continue Façade (FCCS)”, supported by "PO FERS Sicilia 2007/2013 Research line 4.1.1.1", are presented.

This paper has the following structure. After the introduction, in the second paragraph a brief discussion on the LCA analysis of building integrated/ applied solar thermal systems is proposed. The third paragraph illustrates the methodologies and the structure of the project in TRNSYS. The fourth and fifth paragraphs describe the study specification and the results of the energy and environmental analysis carried out considering two distinct scenarios: BSTF constructed with FPC or ETC. Finally, a case study of a prototype of a ventilated solar facade added in the building envelope (vBSTF) is presented.

## **2.0 LIFE-CYCLE OF BUILDING INTEGRATED / APPLIED SOLAR THERMAL SYSTEMS**

The LCA can be developed for a single product or for a set of products, such as a solar system. LCA studies allow comparing design alternatives that are different in terms of environmental impacts. A life cycle study is usually segmented into four distinct phases: product, construction, use, and end-of-life. The product phase is relative to the picking up, the transportation and the manufacture of raw materials into products.

The construction phase consists of the transportation of the products to the final destination and the construction-installation processes. The use stage includes energy and water requirements, maintenance, and material substitution. The end-of-life refers to the decommissioning and the waste processing of solar system products.

In order to assess the life-cycle impacts assessment (LCIA) of a solar thermal facade, the energy produced and delivered inside or exported outside the building system must be included.

Fig. 1 shows the typical stages of an LCA study applied to a building integrated/applied solar thermal system.

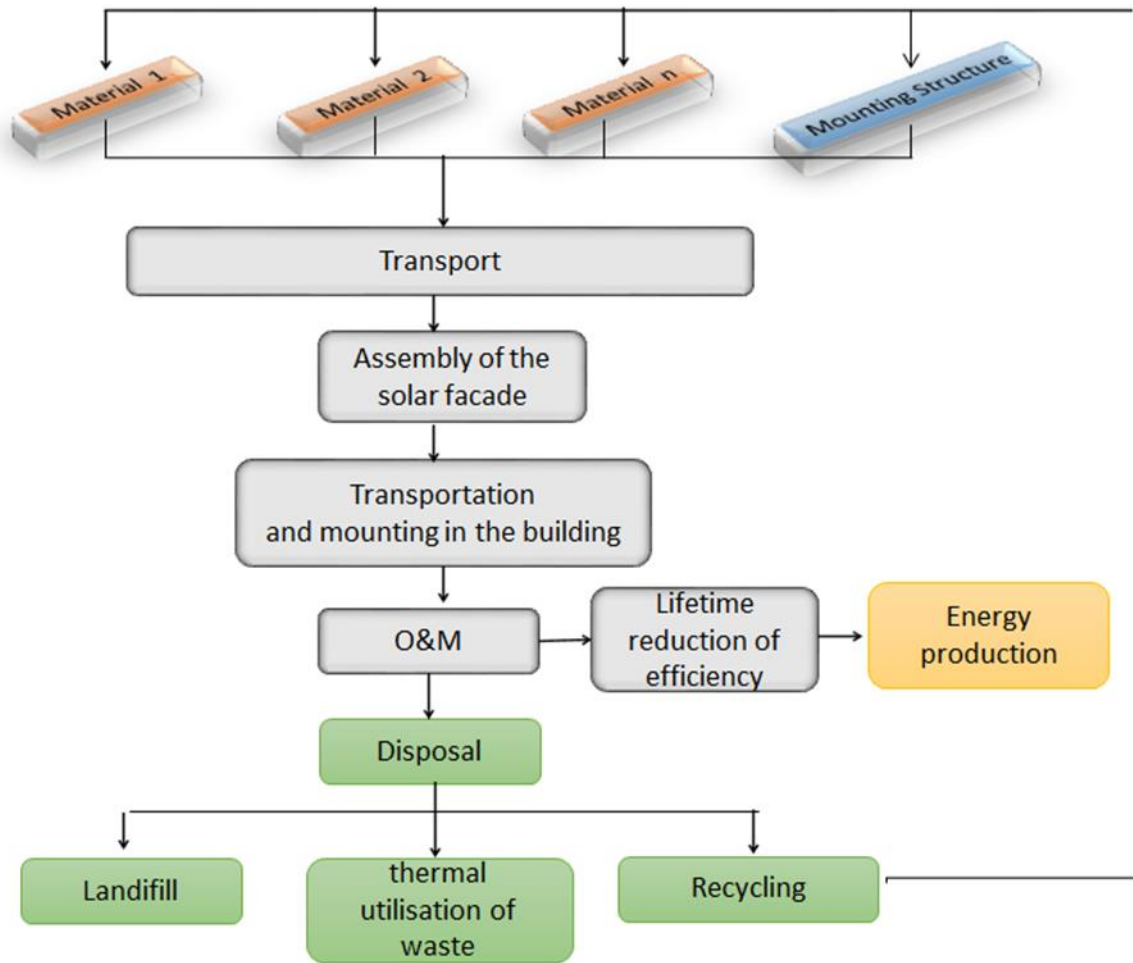


Fig. 1. Typical stages of an LCA study applied to a building-integrated solar thermal system elaborated from [25]

## 2.1 Life-cycle inventory databases.

The life-cycle inventory (LCI) analysis requires the quantification of the inputs of water, energy and raw materials, and discharges to air, land, and water.

The Ecoinvent database is one of the sources most used on LCA studies about building integrated or added façade solar systems by LCA experts.

Life Cycle Environmental Impact Assessment has the aim to assess the potential environmental impacts of the system throughout the life cycle of the product.

Environmental and human health consequences along with resource depletion have to be addressed. The environmental indicators used to evaluate the environmental impacts are: Global Warming Potential (GWP), Ozone Depletion Potential (ODP), Acidification Potential (AP); Eutrophication Potential (EP); Photochemical Ozone Creation Potential (POCP); Abiotic Depletion Potential of Fossil resources (ADP\_FF); Embodied Renewable energy (ER).

A broad LCIA study was conducted in [25] for the average solar technologies available in Switzerland by using SimaPro 7.3 software and Ecoinvent 2.2 database. Tables 1 summarizes the environmental impacts and the energy used to produce 1.0 m<sup>2</sup> of FPC and ETC solar collectors and one piece of different building added solar systems.

Table 1. LCIA of solar collectors and building added solar systems (redrafted from [25])

	Life-cycle impact category	Embodied Energy
--	----------------------------	-----------------

Solar thermal collectors/systems	ADP	GWP [kg CO <sub>2</sub> equiv.]	ODP [kg CFC-11 equiv.]	AP [kg SO <sub>2</sub> equiv.]	POCP [kg C <sub>2</sub> H <sub>4</sub> equiv.]	EP [kg PO <sub>4</sub> equiv.]	ADP_FF [MJ equiv.]	ERE [MJ equiv.]
	Flat plate collector	6.81E-01	1.02E+02	9.69E-06	9.76E-01	5.00E-02	6.65E-01	1.52E+03
Evacuated tube collector	6.74E-01	9.03E+01	8.42E-06	7.81E-01	3.26E-02	6.55E-01	1.48E+03	1.38E+02
Solar system, flat plate collector, one-family house, domestic hot water	9.83E+00	1.33E+03	1.35E-04	8.77E+00	6.24E-01	5.93E+00	2.13E+04	2.55E+03
Solar system, flat plate collector, one-family house, combined system	1.95E+01	2.74E+03	3.52E-04	1.98E+01	1.34E+00	1.39E+01	4.35E+04	5.29E+03
Solar system with evacuated tube collector, one-family house, combined system	1.77E+01	2.35E+03	3.06E-04	1.58E+01	1.03E+00	1.25E+01	3.90E+04	3.68E+03

Carlsoon et al [26] developed a comprehensive environmental analysis of solar systems using the Eco-indicator 99 (EI99)[27], IPCC<sub>100a</sub>[28] as well as the cumulative energy demand indicator (CED). Table 2 summarizes some of the results presented in [26]

Table 2. Environmental analysis of solar systems (redrafted from [26])

Solar thermal collectors/systems	Eco-indicator 99 EI99 (pt)	IPCC <sub>100a</sub> (kg CO <sub>2</sub> eq)	cumulative energy demand CED (GJ)
Flat plate collector	17.2 (7.8) <sup>R</sup>	89 (54) <sup>R</sup>	1.6 (1.0) <sup>R</sup>
Evacuated tube collector	15.3 (8.4) <sup>R</sup>	74.59 (72.5) <sup>R</sup>	1.46 (1.4) <sup>R</sup>
Solar system, FPC (12.8 m <sup>2</sup> ); storage 1.0 m <sup>3</sup>	418 (262) <sup>R</sup>	2539 (1891) <sup>R</sup>	67.6 (54.9) <sup>R</sup>
Solar system, ETC (8.2 m <sup>2</sup> ); storage 1.0 m <sup>3</sup>	318 (226) <sup>R</sup>	1912 (1696) <sup>R</sup>	57.0 (51.5) <sup>R</sup>

<sup>R</sup> Use of 100% secondary metals as an alternative to primary metals

The IPCC 100a indicates the number of greenhouse gases emitted into the atmosphere during the production of one energy unit (e.g. kg CO<sub>2,eq.</sub> per 1 MJ of energy produced).

The Eco-indicator 99 method assesses the environmental effects in terms of damage to human health, ecosystem quality, and resources and it is expressed in points (pt.)

The cumulative energy demand indicator represents the energy necessary for system material/component manufacture, installation, material disposal, and transportation during all the life cycle phases.

The above-mentioned studies [25] and [26] provide quite similar results in regard to the emission of CO<sub>2</sub> (kg CO<sub>2,eq</sub>), respectively indicated in terms of GWP and IPCC<sub>100a</sub>.

Substantial correspondences are found between the values of ADP\_FF and CED.

In the light of the previous scrutiny, it is possible to assume that data in table 1 and 2, in accordance with [25], are valid at European scale “ given the fact that there are only slight differences between the technologies used within the European countries”.

Moreover, it is worth emphasizing that the environmental performance of FPC and ETC differed significantly. The production and installation of an ETC solar system determine life-cycle impacts lower than that one of an equivalent FPC solar system.

Metallic copper and aluminum make the largest contribution to the environmental load for solar collectors. However, if secondary metals are used, the contribution to the environmental load of the metallic part of the solar collectors are significantly reduced.

### 3.0 METHODOLOGY

In this section, firstly the solar thermal system is illustrated, then the TRNSYS model is presented.

#### 3.1 Description of the simulated solar plant

The thermal energy produced by the solar collectors is transferred to the solar storage tank and then used for DHW production (see fig. 2). An auxiliary heater will provide the necessary energy for heating up the water in order to reach the set-point temperature (45°C).

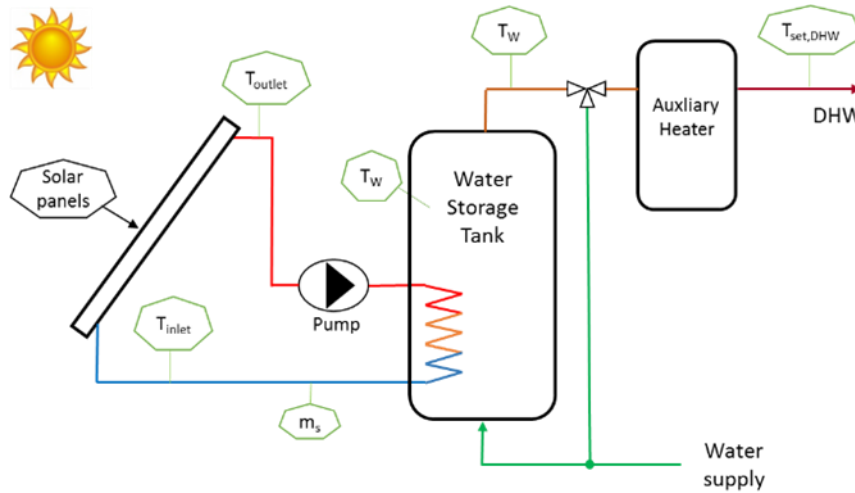


Figure 2. Scheme of the solar system

The thermal power “ $P_{th}$ ” transferred from the solar collectors to the storage tank is calculated by equation (1), as a function of the mass flow rate  $m_s$ , the water specific heat  $C$  and the difference between the inlet and the outlet temperatures in the storage tank.

$$P_{th} = m_s \cdot C \cdot (T_{in} - T_{out}) \quad (1)$$

The thermal efficiency of the solar collectors is calculated, in accordance with the European standard EN 12975, by equation (2).

$$\eta_{th} = \eta_0 - a_1 \cdot \frac{(T_m - T_a)}{G_k} - a_2 \cdot \frac{(T_m - T_a)^2}{G_k} \quad (2)$$

where  $\eta_0$ ,  $a_1$  and  $a_2$  are the parameters that characterize the solar panel, while  $T_m$ ,  $T_a$ , and  $G_k$  are respectively the average temperature of solar panel, environmental air temperature and incident solar radiation.

Energy provided by the auxiliary ( $E_{aux}$ ) is calculated by:

$$E_{aux} = \int \dot{m}_w \cdot C \cdot (45 - T_w) \cdot dt \quad (3)$$

where  $m_w$  is the flow rate of DHW required by the user and  $T_w$  is the temperature of the water at the outlet of the storage tank.

Then, the valuable energy produced by the solar system is determined by the difference between the energy demand for DHW production ( $E_{DHW}$ ) and the energy supplied through the auxiliary heater [A Gagliano, GM Tina, S Aneli, S Nižetić ,Comparative assessments of the performances of PV/T and conventional solar plants Journal of Cleaner Production].

$$E_{th} = E_{DHW} - E_{aux} \quad (4)$$

The fraction of the energy demand for DHW production supplied by the solar systems is evaluated by:

$$f = \frac{E_{DHW} - E_{aux}}{E_{DHW}} \quad (5)$$

### 3.2 TRNSYS simulations

The model of the solar system created in TRNSYS software [29] through the graphical user interface ‘Simulation Studio’, consists of various components organized by joining the outputs of the one to the input(s) of the other(s).

Thus, distinct components describe the solar thermal loop (i.e. solar panels, storage tank, unit pump, and controller) as well as the management of the energy demand (i.e. DHW load, thermal mixing, auxiliary heater).

Inputs and outputs parameters are the temperatures of the fluid at the inlet/outlet of the solar collectors, the solar panel thermal efficiency, the temperature in the thermal storage, the auxiliary energy demand. Figure 3 shows the flow diagram of the solar system created in TRNSYS.



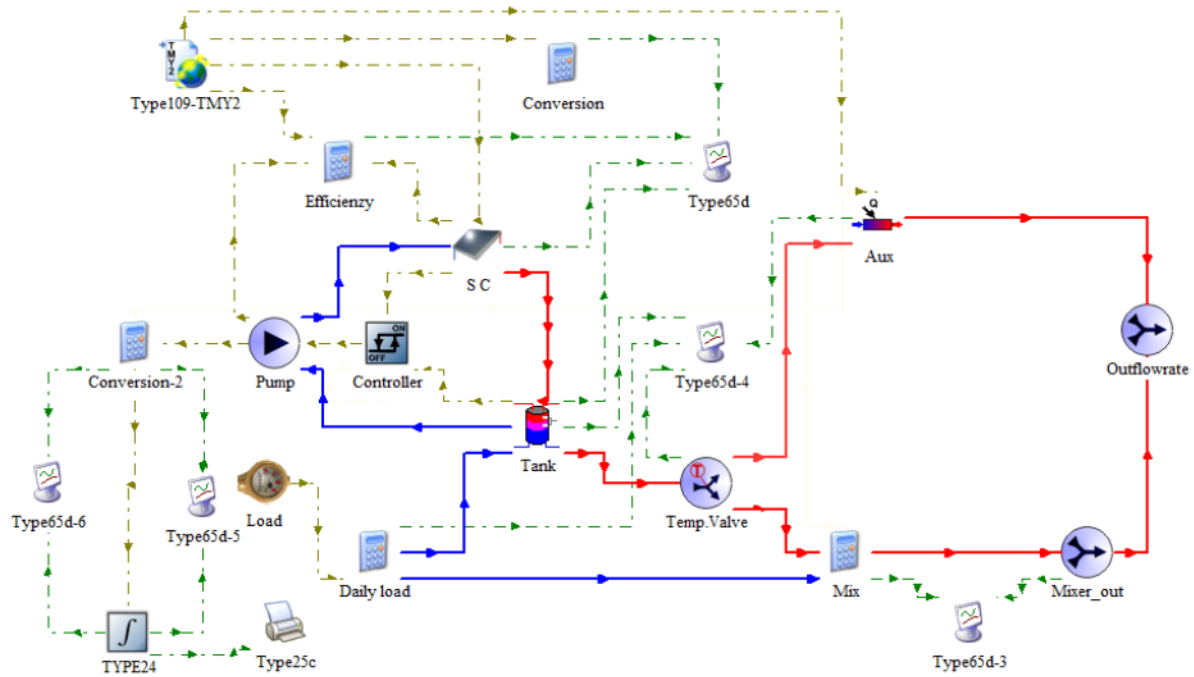


Figure 3. TRNSYS assembly of the simulated solar system.

The solar collector receives hourly meteorological data as inputs from the Type 109 data reader in the standard TMY2 format. The On/Off controller receives inputs of the fluid temperature that exits the collector and the temperature of the fluid at the bottom of the storage tank. The output control function is connected with the pumps, thus switching it on or off, allowing or not the charging of the tank (Type 60).

The DHW tank subsystem includes the components that define the request for DHW (Type 4c), as well as a temperature-controlled flow diverter (Tempering Valve - Type 11b) used to regulate the flow stream at the required temperature  $T_{set}$ . When the enthalpy level from the solar tank is insufficient for achieving the minimum required temperature, the flow stream goes to the auxiliary heating system.

As previously explained two distinct BSTF configurations are simulated, in the first the solar collectors used are flat plate model (scenario 1), while in the second configuration the solar collectors used are evacuated tube model (scenario 2).

Consequently, Type 1 describes the solar collector subsystem, under scenario 1, while Type 71 describes the evacuated tube collector, under scenario 2.

#### 4.0 STUDY SPECIFICATIONS

In this section of the study, the results of the simulations of a BSTF (tilt angle of  $90^\circ$ ), facing South, located in four different Italian cities, that are Ragusa, (lat  $36^\circ 55'$ ) Catania (lat.  $37^\circ 30'$ ), Rome (lat.  $41^\circ 53'$ ) and Milan (lat.  $45^\circ 28'$ ), are illustrated.

The analyses carried out evaluate the fraction of DHW energy demand that can be satisfied through BSTF constructed with two distinct typologies of solar collectors, FPC (scenario 1) and ETC (scenario 2), under different climatic conditions.

In both scenarios, the BSTFs have an area of  $4.0 \text{ m}^2$ , which was chosen as a reference for an Italian residential unit with a DHW consumption of about 200 l/day. The hourly consumption profile is that suggested by the standard EN 15316:2007.

Table 3 shows the technical data of commercial solar collectors available in the Italian market that were used in the simulations.

Table 3. features of the two typologies of thermal collectors

Panel type	$\eta_0$ (-)	$a_1$ (W/m <sup>2</sup> K)	$a_2$ (W/m <sup>2</sup> K <sup>2</sup> )
Glazed flat plate	0.803	3.550	0.035
Evacuated-tube	0.789	1.550	0.007

The climatic differences among the four cities are shown in figures 4 and 5.

Figure 4 depicts the average monthly temperatures (a) and the heating degree days (HDD) (b).

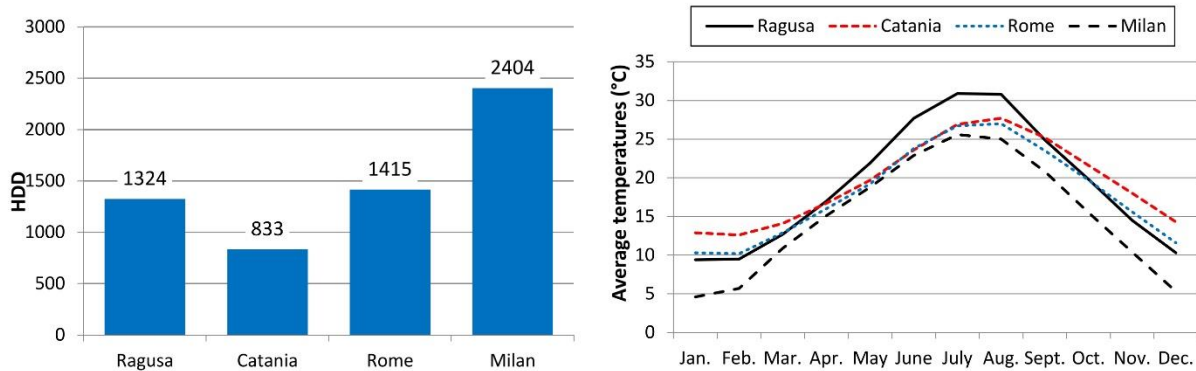


Figure 4 . Heating Degree Day (left-side); average monthly temperatures (right-side)

The greatest differences of temperature among the cities emerge during the winter period, up to 10°C between Milan and Catania is observed.

The climatic differences among the cities can be highlighted through the Heating Degree Day, Milan has the highest HDD (2404), which are about two times higher than that one of Rome and Ragusa (1415 and 1324) and almost three times the HDD of Catania (833).

Moreover, the highest temperature is reached in the city of Ragusa during the summer.

Figure 5 depicts the global solar irradiance that hits a vertical surface in the winter and summer solstices under clear sky conditions [30].

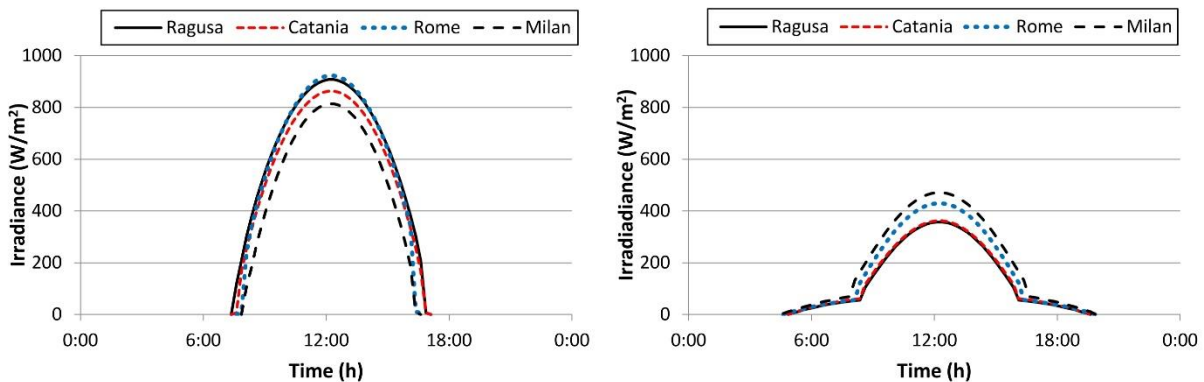


Figure 5. Solar radiation on winter solstice (left-side) and summer solstice (right-side).

The solar irradiance on a south-facing vertical solar façade on a sunny winter day is higher than the solar irradiance on a sunny summer day. Actually, the maximum winter solar irradiance is even twice the maximum solar irradiance in summer days.

The solar irradiance has quite modest differences among the four cities both in winter and summer days. This means that such position of the solar collectors smooths the dependence of the solar

radiation by the latitude. During summer days, the solar irradiance reaches the highest values in Milan and the lowest in Catania and Ragusa, so the cities with the lesser latitude are the most penalized during the hot season.

Figure 6 shows the solar radiations collected by the vertical solar façade during all year round in the investigated cities.

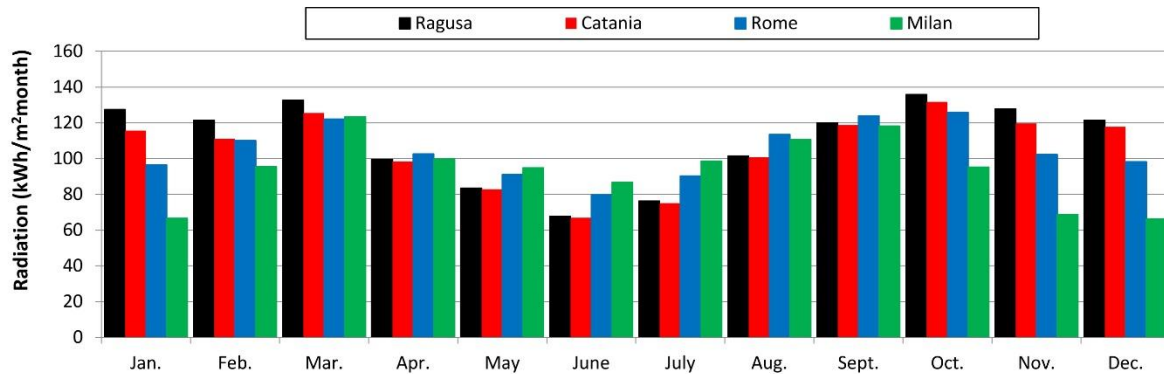


Figure 6. Comparison of monthly solar radiation

As previously observed, the values of solar radiation do not reach the highest values during the summer months, except for Milan. More specifically, the solar radiation in Ragusa, Catania, and Rome in June is less than the solar radiation in December of about 46%, 42% and 17%.

In these cities, the highest monthly solar radiations are achieved during the spring and autumn months.

respectively. During the summer period a vertical solar façade has modest performance especially in the sites with the lowest latitudes. Milan, which is the further north city, has greatest values of monthly solar radiation from May to July.

During the winter months, the solar radiation that strikes a vertical surface reach  $90^\circ$  has the highest value, so improving the performance of the solar system. However, in Milan, due to its worst meteorological conditions the solar radiation has the lowest values.

## 5.0 SIMULATION RESULTS

In this section, some of the results of transient simulations carried out for the two scenarios are shown and commented.

It has to be underlined that in this study the interactions between the solar thermal facade and the building energy load are neglected.

### 5.1. Winter period

The results of transient simulations allow determining per each month, city and scenario all the data that characterize the functioning of a BSTF.

As an example, the results obtained during a winter week (January 20-27) in Ragusa and Milan, which respectively could be assumed as representative for temperate and cold climate, are shown in the following.

Figures 7 depicts the outlet temperatures from the solar collectors under scenario 1 ( $T_{o,s1}$  dotted red line) and scenario 2 ( $T_{o,s2}$  dotted light blue line), the ambient air temperatures ( $T_a$ , green line), the solar irradiance ( $I_\beta$ , black line), as well as the temperatures in the solar tank ( $T_{s1}$ , red line and  $T_{s2}$  light blue line), in Ragusa.

Figure 8 shows the same parameters in Milan.

During this week, it is possible to observe the effect of different sky conditions on the thermal behavior of these solar systems.

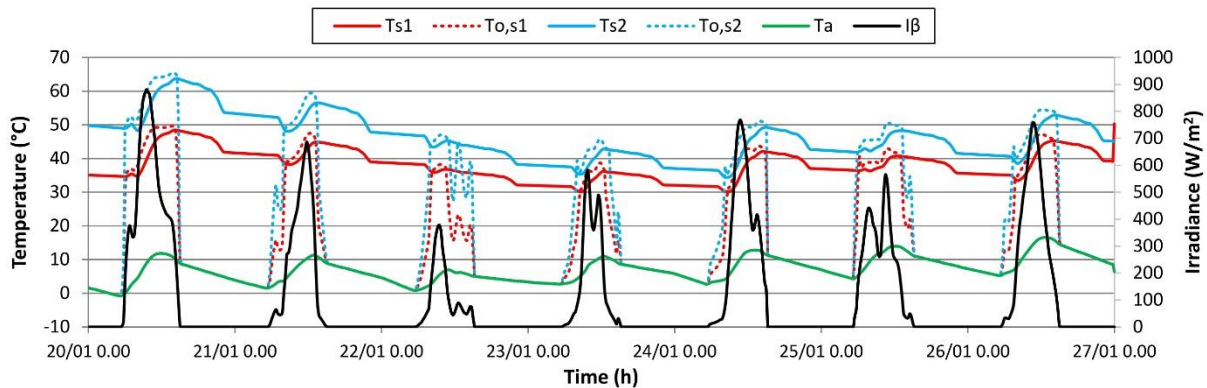


Figure 7. Solar tanks temperatures and weather-data during a winter week in Ragusa.

As regards Ragusa, under scenario 1 the temperatures in the solar tank,  $T_{S1}$ , are constantly higher than  $30^{\circ}\text{C}$ , with the highest values that do not exceed  $50^{\circ}\text{C}$ .

Under scenario 2 the temperatures in the solar tank,  $T_{S2}$ , are constantly higher than  $35^{\circ}\text{C}$ , with the highest values that do not exceed  $65^{\circ}\text{C}$ .

The daily variation of the temperatures in the solar tank is quite similar in both scenarios with differences of almost  $10^{\circ}\text{C}$ , during the whole period.

Analogous considerations may be pointed out for the outlet temperatures from the solar collectors, it is confirmed that  $T_{o,s2}$  is always higher than  $T_{o,s1}$ .

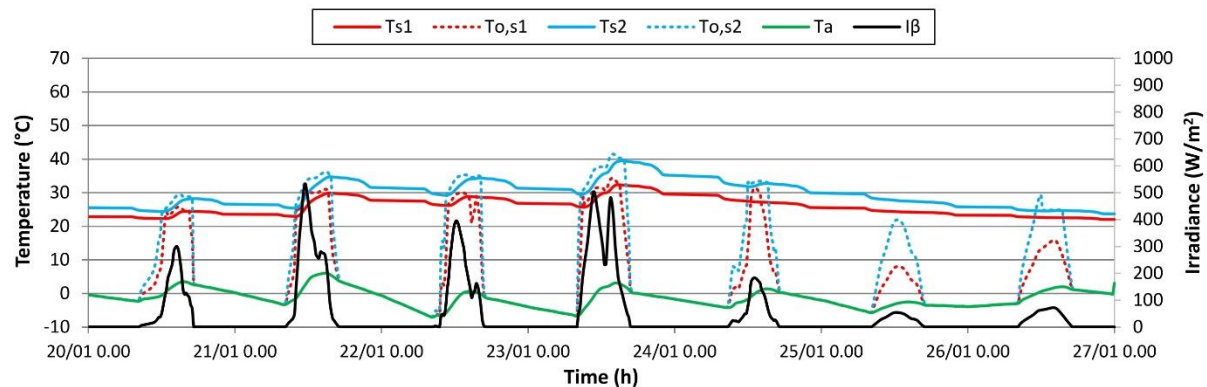


Figure 8. Solar tanks temperatures and weather-data during a winter week in Milan.

As regards Milan, during the same observed winter week the solar irradiance as well as the outdoor temperatures are lower than that in Ragusa.

In particular, the last three days represent very cloudy sky conditions for which only the diffuse component of the solar radiation is present. Consequently, the two solar systems do not produce any useful energy.

Once again, the daily variation of the temperatures in the solar tank during the whole period are quite similar in both scenarios.

Thus, comparing equivalent scenarios, a BSTF installed in Ragusa allows reaching solar tank temperatures that are at least  $10^{\circ}\text{C}$  higher than that attained in Milan.

Figure 9 shows, for both scenario1 and 2, the hourly thermal energy provided by the solar plants ( $E_{th}$ ) and that one supplied by the auxiliary heater ( $E_{aux}$ ) installed in Ragusa. Figure 10 shows the same parameters in Milan.

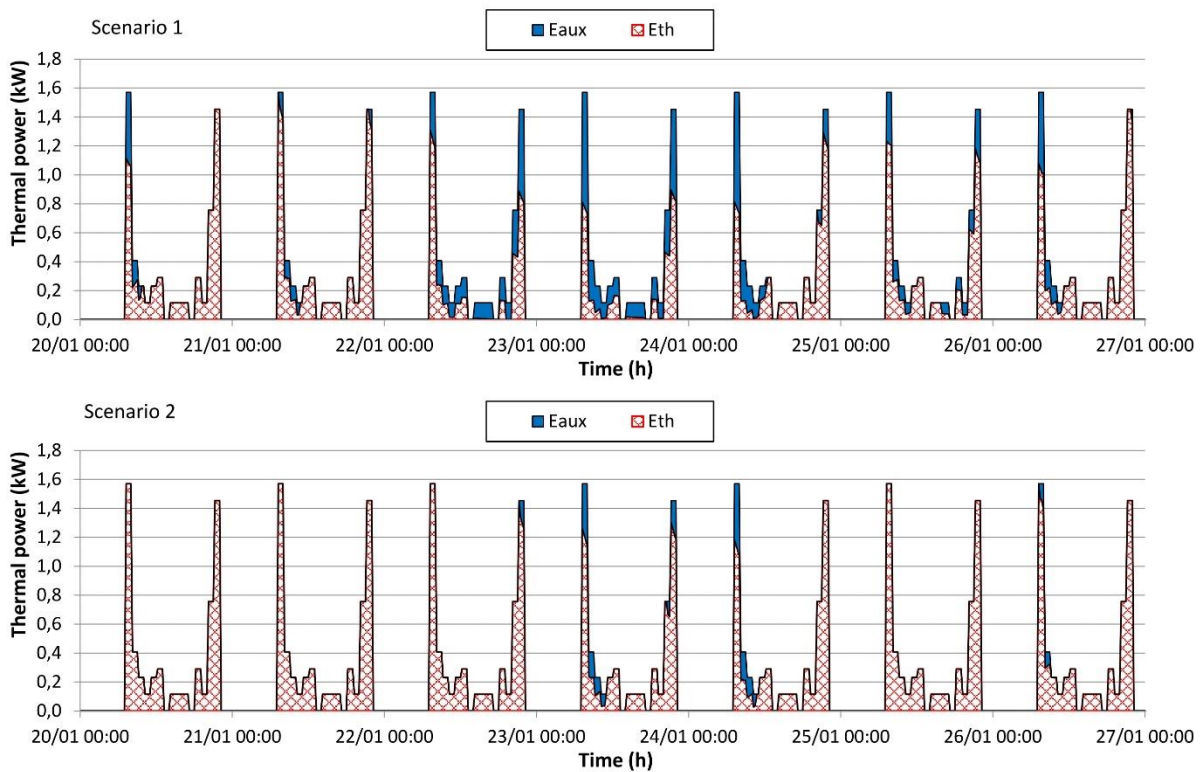


Figure 9. Energy fluxes during a winter week in Ragusa.

In the above graphs, the areas subtended by the curves correspond to the daily energy needs for DHW production.

Under scenario 1, although the energy supplied by the solar system guarantees great daily coverage factors, higher than 0.7, the auxiliary heater has to function all the days. In particular in the morning and in the late hours of the day.

Otherwise, under scenario 2 the daily coverage factors significantly increase. In fact, during four days the DHW energy requirements are totally supplied through the solar system ( $f = 1.0$ ), and in the other three days, the energy supplied by the auxiliary heater is very small.

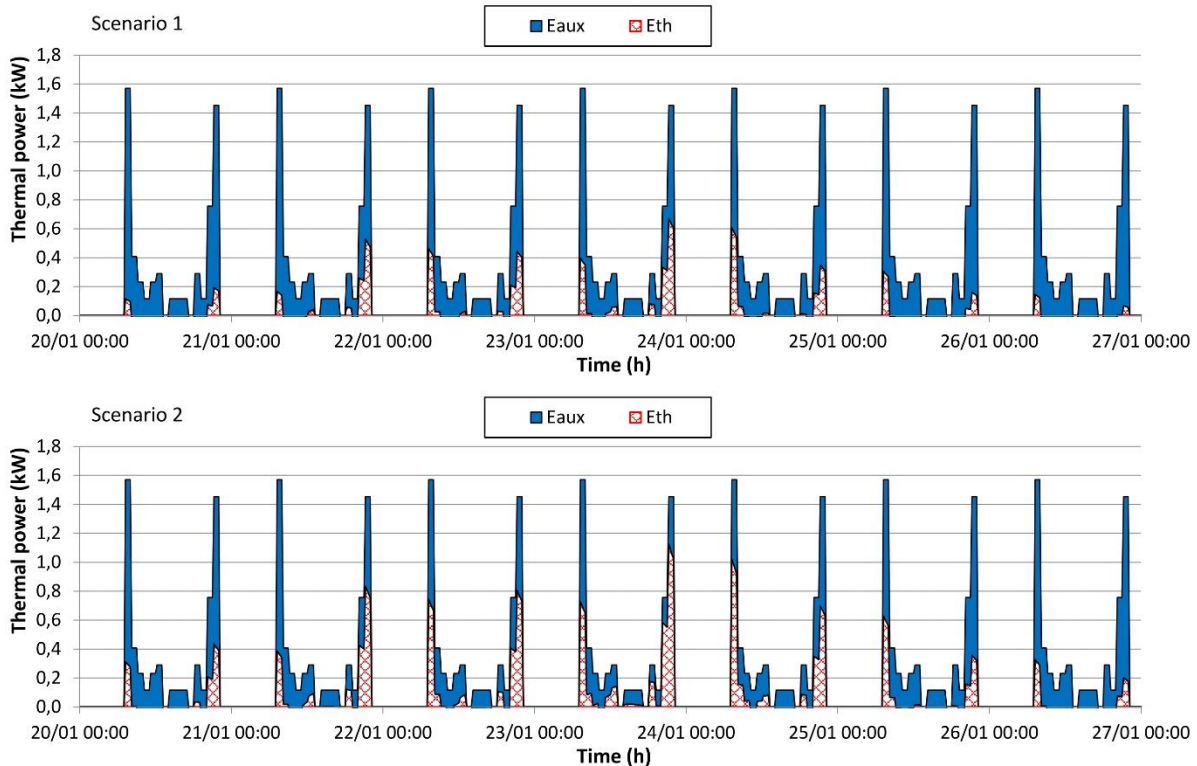


Figure 10. Energy fluxes during a winter week in Milan.

The performances of the BSTF installed in Milan are modest compared with that one of Ragusa. In particular, under the scenario 1 the thermal power supplied by the solar plant is very scarce, just in one day the solar system provides of about 0.65 kW that is about 40% of the peak value for the DHW demand.

Under scenario 2, the performances of the system, although remain modest, increase significantly reaching a thermal power of about 1.1 kW that is about 70% of the peak value for the DHW demand. This outcome evidences that the ETC solar collectors exploit better their features in the coldest climates.

Generally, the scarce performances obtained from both the two solar systems are related to the low values of solar radiation and air temperatures as previously highlighted.

It is interesting to underline that the energy provided by the solar plant is strictly coupled with the daily trend of the DHW needs, which have peaks values in the early morning and in the late evening.

### 5.1.2 Summer period

Similarly, the same analysis showed for the winter season are proposed in the summer period (20-27 June).

Figure 11 depicts the outlet temperatures from the solar collectors under scenario 1 ( $T_{o,s1}$  dotted red line) and scenario 2 ( $T_{o,s2}$  dotted light blue line), the ambient air temperatures ( $T_a$ , green line), the solar irradiance ( $I_\beta$ , black line), as well as the temperatures in the solar tank ( $T_{s1}$ , red line and  $T_{s2}$  light blue line), in Ragusa.

Figure 12 shows the same parameters in Milan.

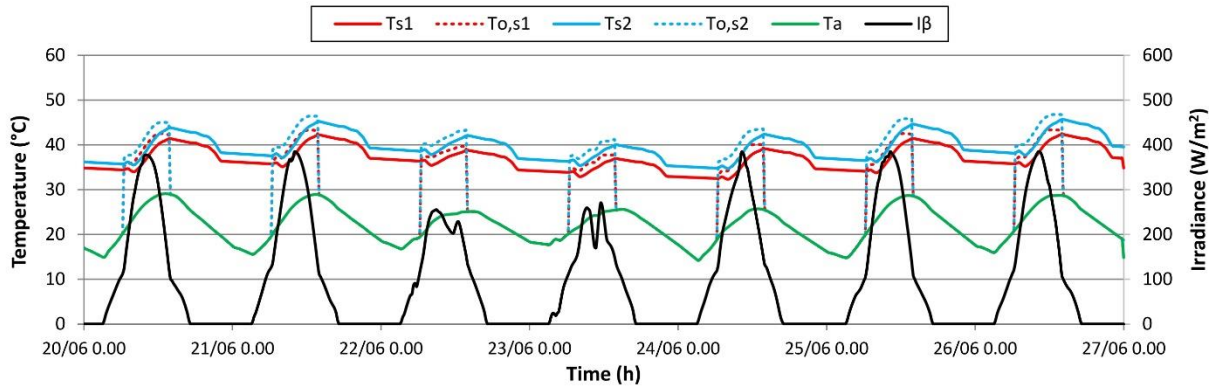


Figure 11. Solar tanks temperatures and weather-data during a summer week in Ragusa.

As regards Ragusa, under the scenario 1 the temperatures in the solar tank,  $T_{S1}$ , ranges from 32 to 42°C, while under the scenario 2,  $T_{S2}$ , ranges from 35 to 45°C.

The daily variation of the temperatures in the solar tank is quite similar in both scenarios with differences less than 5°C, during the whole period.

Analogous considerations may be pointed out for the outlet temperatures from the solar collectors, it is confirmed that  $T_{o,s2}$  is always higher than  $T_{o,s1}$ .

These outcomes confirm that the two BSTFs have energy performances that are not so different between the winter and the summer period in Ragusa.

This is due to the reduced irradiance that strikes a vertical surface south exposed during the summer period. The maximum daily values of irradiance are of about 50% lesser than that observed during a sunny winter day.

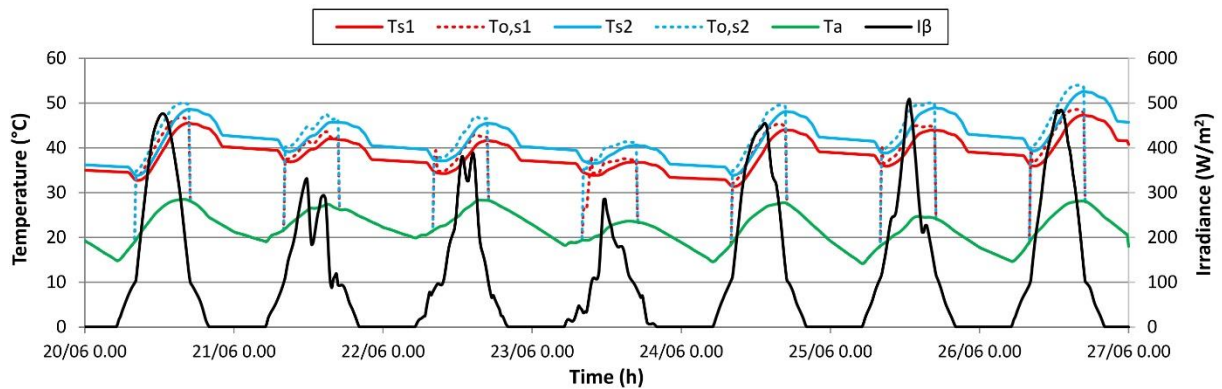


Figure 12. Solar tanks temperatures and weather-data during a summer week in Milan

As regards Milan, during the same observed summer week the solar irradiance that strikes the solar façade is higher than in Ragusa, while the outdoor temperatures are similar.

Once again, the daily variation of the temperatures in the solar tank is quite similar in both scenarios, during the whole period.

Under the scenario1 the temperatures in the solar tank,  $T_{S1}$ , are continuously higher than 32°, with peak values that reach 47°C, while under the scenario2 the temperatures achieved in the solar tank,  $T_{S2}$ , are permanently higher than about 5.0°C respect to the scenario1.

Thereby, rather unexpectedly, the solar tank temperatures in Milan are 5.0 °C higher than that one achieved in Ragusa.

As previously discussed, this outcome indicates that the reductions of the performances of a vertical solar façade are greatest in cities with low latitude (e.g. Ragusa).

Figure 13 shows the hourly thermal power supplied by the solar plants ( $E_{th}$ ) and that one supplied by the auxiliary heater ( $E_{aux}$ ), in Ragusa during the summer week (June 20-27). Figure 14 depicts the same data in Milan.

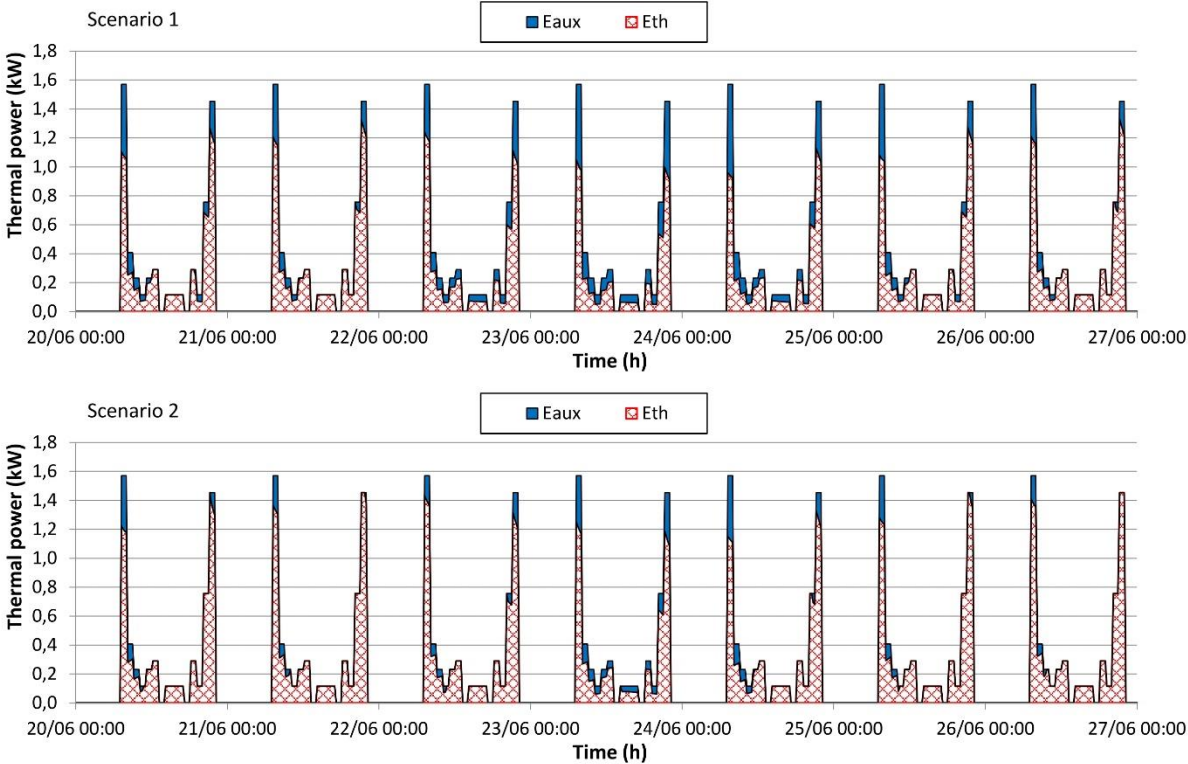


Figure 13. Energy fluxes during a summer week for Ragusa.

Under scenario 1, although the energy supplied by the solar system guarantees great daily coverage factors, higher than 0.8, the auxiliary heater has to function all the days. Under scenario 2 the daily coverage factors further increase, but anyway in all days it is necessary to supply a little amount of energy by the auxiliary heater. These outcomes confirm that the two BSTFs have energy performances that are not so different between the winter and the summer period in Ragusa.



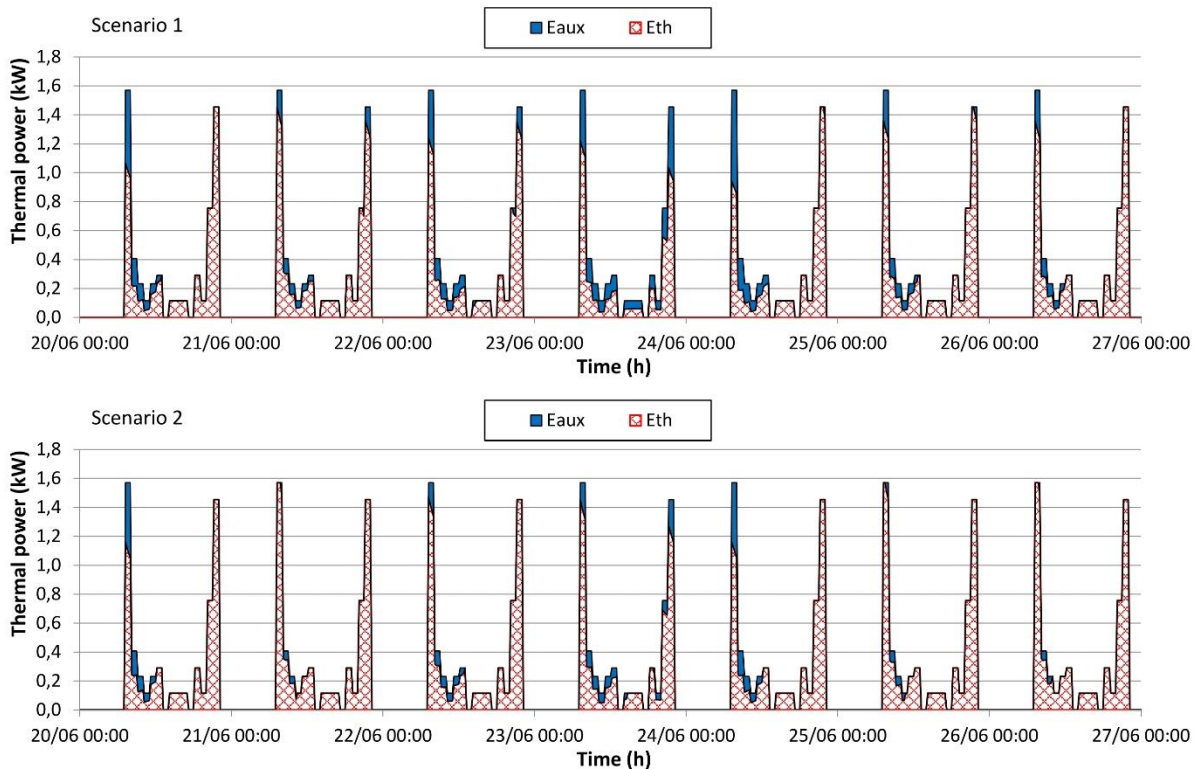


Figure 14. Energy fluxes during a summer week for Milan.

During the summer season, the daily coverage factors show substantial increase respect to the winter season thanks to the high values of the irradiances and of the air temperatures. Under scenario 2 the performances of the BSTF are a bit better respect to scenario 1. Even in Milan, the solar plants do not allow fully balancing the energy demand for DHW. This reveals the mandatory use of an auxiliary energy source. It is worth of interests to underline that during such summer week, the solar plants in Ragusa and Milan achieve almost similar performances.

### 5.1.3 Yearly performances

In this section of the study, the yearly performances of the solar façade are presented. Figure 15 shows the monthly coverage factor values “f” for both the scenarios analysed.

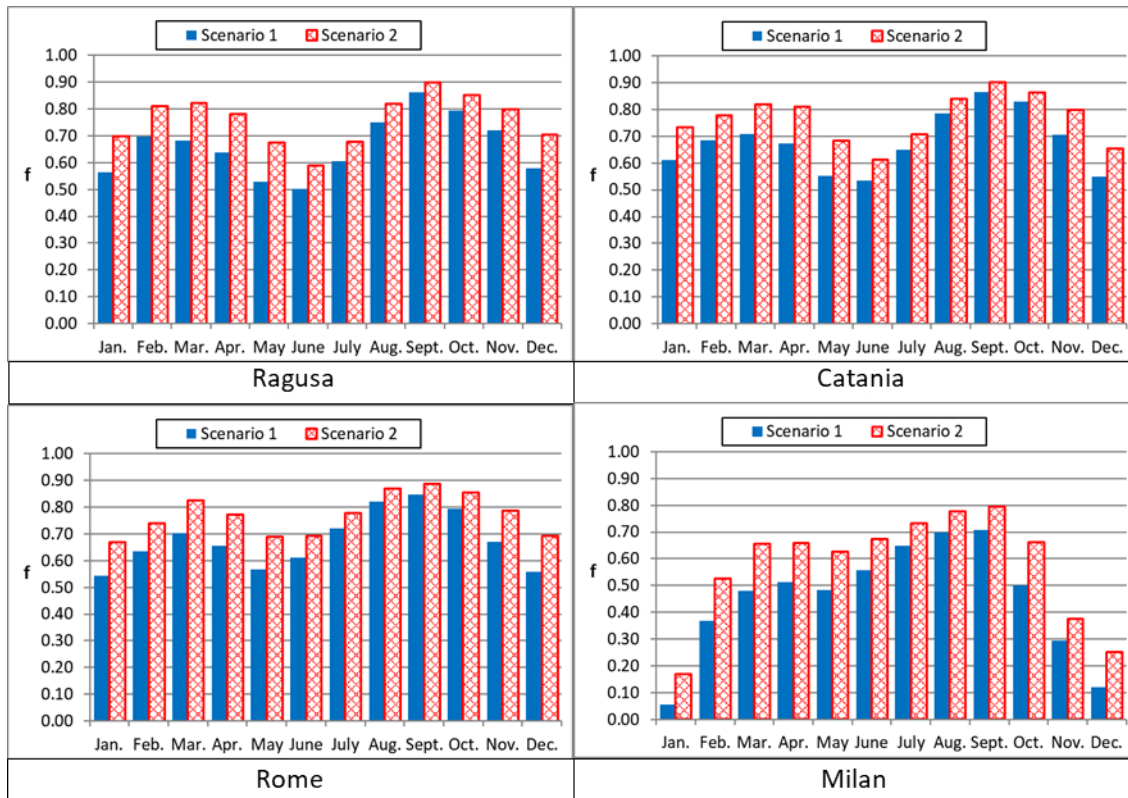


Figure 15. Coverage factor of DHW demand for the two scenarios.

It can be observed that the coverage factors “f” in Catania, Ragusa, and Rome are quite similar during the whole year. As regard, Milan, under scenario 1 the coverage factor “f” has modest values during the winter period. Coverage factors less than 10% are achieved during the coldest months. Otherwise, under scenario 1 during the mid and the summer seasons the coverage factors “f” reach values of about 0.60, while under scenario 2 a value of about 0.70 is achieved.

As expected, the higher values of “f” are reached during the mid-season and the use of the ETC allows achieving the highest performance.

It is important to note that solar systems installed on the south-facing façade allow reducing the fluctuations of the coverage factor throughout the year, especially when evacuated tube collectors are used. Moreover, during the summer, the reduced solar irradiance that hits the vertical surfaces avoids overproduction and therefore energy waste.

Table 4 shows the yearly thermal energy supplied by the solar panels ( $E_{th}$ ), the auxiliary energy supplied by the auxiliary system ( $E_{aux}$ ) as well as the coverage factor (f), for the different scenarios and cities. The percentage differences in the energy yields between the two scenarios are also indicated.

Table 4. Annual result for the analyzed scenarios

	Scenario 1			Scenario 2			% Difference		
	$E_{th}$ (kWh)	$E_{aux}$ (kWh)	f (-)	$E_{th}$ (kWh)	$E_{aux}$ (kWh)	f (-)	$\Delta E_{th}$	$\Delta E_{aux}$	$\Delta f$
Ragusa	1943	1028	0.65	2247	724	0.76	15.6	-29.5	15.6
Catania	1999	972	0.67	2263	708	0.76	13.2	-27.2	13.2
Rome	1994	977	0.67	2281	690	0.77	14.4	-29.3	14.4
Milan	1312	1659	0.44	1685	1286	0.57	28.4	-22.5	28.4

In Ragusa, Catania, and Rome a vertical BSTF constructed with 4.0 m<sup>2</sup> of flat plate collectors allows to satisfy up to 65% of the energy needs for DHW requirements. On the other hand, in Milan just about 44.0% of the DHW demand is satisfied. This quite modest outcome is due to multiple factors, such as limited solar radiation, cool air temperatures and few days with clear sky compared to the other cities, during the winter months.

The use of ETC improves the performances of the solar facades of about 15.0 % in Ragusa, 13.0% in Catania and 14.0% in Rome, it allows reaching a yearly “f” factor of 0.76.

In Milan, where the coldest climate limits the efficiency of flat plate collectors, the use of ETC allows boosting the yearly “f” factor up to 0.57 with an increment of 28.0%.

It is possible to highlight that the differences among the performances of the solar facades are not directly related to the values of the HDD. Indeed, in Ragusa and Roma, the coverage factor is about the same of Catania, although the HDD of Ragusa and Roma are about 1.5 times the number HDD of Catania.

The accuracy of the results obtained through TRSNYS software is proved by numerous literature studies.[31] [32]

#### 5.1.4 Economic analyses

In this section, a simplified economic analysis of the two alternatives is proposed. In particular, the Payback time (PBT) due to the extra expenses necessary for installing the ETC into the BSTF solar façade, as they have costs higher than that of the flat plate collector, has been calculated. A difference of cost between the two typologies of the solar collectors ( $\Delta C$ ) of 120,00 Euro/m<sup>2</sup> has been evaluated.

PBT is calculated as:

$$PBT = \frac{\Delta C}{ES_{ETC} - ES_{FPC}} \quad (7)$$

where

$\Delta C$  is the cost difference between ETC and FPC (Euro)

$ES_{ETC}$  is the economic saving under scenario 2 (ETC)

$ES_{FPC}$  is the economic saving under scenario 1 (FPC)

For each scenario, the economic savings ES has been calculated by the product of  $E_{th}$ , (shown in table 4) per the cost of the thermal energy, assumed 90,00 €/MWh.

The difference between the energy saving achievable by the two systems ( $\Delta ES$ ) determines the payback time necessary for compensating the extra expenses necessary for installing the ETC into the BSTF. Table 5 summarizes the main outcomes of this analysis.

Table 5. Economic comparison between the two scenarios.

	<i>Scenario 1</i>	<i>Scenario 2</i>	<i>Difference</i>	<i>Payback time</i>
	$ES_{FPC}$ (€/y)	$ES_{ETC}$ (€/y)	$\Delta ES$ (€/y)	year
Ragusa	174,87	202,23	27,4	17.54
Catania	179,91	203,67	23,8	20.20
Rome	179,46	205,29	25,8	18.58
Milan	118,08	151,65	33,6	14.30

The installation of the evacuated tube solar collectors (ETC) instead of the flat plate collectors (FPC) involve payback times of about 20 years in Catania, and of about 18 years in Ragusa and Roma meanwhile in Milan the payback time is less than 15 years.

These outcomes highlight that the use of the ETC has the best economic feasibility in Milano, under the current financial scenario.

Thus, the use of the ETC in BSTF system could be suggested in localities that has HDD of about 2400, that are the values of the HDD in Milan.

### 5.1.5 Energy and emission payback times

In this section of the study, the energy and emission payback time are calculated using the literature data showed in [26].

The energy payback time (EPBT), defined as the time necessary for a solar installation to ‘pay back’ the same amount of energy equivalent to that required for the production /operation of the renewable plant itself [22], is calculated as:

$$E_{PBT} = \frac{E_{in}}{E_{useful} - E_{O\&M}} \quad (8)$$

where

$E_{in}$  is the primary energy needed for system material/component manufacture, installation, material disposal, and transportation during all the life cycle phases (GJ);

$E_{useful}$  is yearly energy output of the solar thermal system (GJ per year);

$E_{O\&M}$  is the energy consumed during the use phase of the solar thermal system (GJ per year).

The overall impacts of the solar system during its life cycle and the emission savings are assessed through the emission payback-time ( $EM_{PBT}$ ).  $EM_{PBT}$  is the time for a solar installation to avoid the same amount of emissions equivalent to that required for the production /operation of the renewable plant itself for the generic pollutant.

The emission payback-time related to  $CO_{2eq}$  emission is calculated by the following equation:

$$EM_{PBT,CO_{2eq}} = \frac{EM_{CO_{2eq}}}{EM_{s,CO_{2eq}} - EM_{O\&M,CO_{2eq}}} \quad (9)$$

where

$EM_{CO_{2eq}}$  is the global emissions of  $CO_{2eq}$  related to the production, assembly, transport, maintenance and disposal of the solar plant ( $kg_{CO_{2eq}}$ );

$EM_{s,CO_{2eq}}$  is the yearly emission saving of  $CO_{2eq}$ . ( $kg_{CO_{2eq}}/year$ );

$EM_{O\&M,CO_{2eq}}$  is the yearly emission of  $CO_{2e,q}$  related to the use of the renewable plant ( $kg_{CO_{2eq}}/year$ ).

The data necessary for calculating  $E_{PBT}$  and  $EM_{PBT}$ , which are IPCC<sub>100a</sub> and CED were derived from [26]. Since the actual volume of the solar tank installed in the investigated systems (0.4 m<sup>3</sup>), is different by the reference solar tank (1.0 m<sup>3</sup>), it was introduced the corrective factor  $1/2.5^{0.5}$  for calculating the number of materials employed.

The amount of aluminum in the collector frames was assumed proportional to the solar collector area.

Table 6 shows the IPCC<sub>100a</sub> and CED for the two solar systems under investigation.

Table 6. IPCC<sub>100a</sub> and CED for the two solar systems under investigation

Solar thermal collectors/systems	IPCC <sub>100a</sub> (kg CO <sub>2,eq</sub> )	Cumulative energy demand CED (GJ)
BSTF - FPC (4.0 m <sup>2</sup> ); storage 0.4 m <sup>3</sup>	1074	18.5
BSTF - ETC (4.0 m <sup>2</sup> ); storage 0.4 m <sup>3</sup>	917	7.36

Data reported in table 7 have been calculated under the following assumptions.

The energy consumed during the use phase of the solar system ( $E_{O\&M}$ ), which is estimated in 0.75 GJ/year, as well as yearly emission of CO<sub>2,eq</sub> related to the use of the renewable plant ( $EM_{O\&M,CO_{2,eq}}$ ) is not included in the two environmental descriptors.

The yearly emission savings ( $E_{MS,CO_{2,eq}}$ ) are calculated evaluating the emissions of a conventional system (e.g. a domestic gas boiler) that delivers as much energy as that supplied by the solar system. Thus, for domestic gas boilers, a global warming factor of 215 g CO<sub>2,eq</sub> per kWh of useful heat [33] is assumed.

The yearly emissions of CO<sub>2,eq</sub> ( $EM_{O\&M,CO_{2,eq}}$ ) deriving by the use of the renewable plant, descends by the electricity consumed by the pumps, which were calculated adopting a specific emission of 287 g CO<sub>2,eq</sub> per kWh [31].

Table 7. Energy and environmental payback time per the two solar facades.

	<i>Scenario 1</i>	<i>Scenario 2</i>	<i>Scenario 1</i>	<i>Scenario 2</i>
	$E_{PBT}$	$E_{PBT}$	$EM_{PBT}$	$EM_{PBT}$
Ragusa	2.96	1.00	2.75	2.01
Catania	2.87	0.99	2.67	2.00
Rome	2.88	0.99	2.68	1.98
Milan	4.66	1.38	4.22	2.74

The energy payback-time related to the scenario1 (FPC) is higher than the energy payback-time of scenario 2 (ETC). This result depends not only by the greatest energy supplied by the ETC but also and mainly on the fewer primary energy needed for system materials/components assembly. Scenario 2 allows attaining EPBTs that are always lesser than 1.4 years, while scenario 1 has EPBTs that are of about 3.0 years and even more than 4.5 years in Milan.

As regard, the emission payback times the differences between the two scenarios are smaller. Scenario 2 confirms the best performances, with EPBTs that are lower than 2 years with the exception of Milan that has an EPBT of about 2.7 years. Once again, under scenario 1, Milan has an EPBT higher than 4 years.

Evidently, the use of secondary metals as an alternative to primary metals reduces the environmental impact of the FPC collectors smoothing the disproportion between the environmental impacts of the two solar technologies.

However, both the two solar façades have short energy and emission payback times in comparison with the life cycle of a solar system that is at least 20 years. Thus, the positive judgments, revealed by the short payback times values for both energy and CO<sub>2</sub>, allow affirming that vertical solar façades represent suitable systems for DHW production with great environmental convenience.

## 6.0 EXPERIMENTAL v-BSTF PROTOTYPE

In this section, the prototype design and data collected through the monitoring system are illustrated

### 6.1 Prototype design

Under the research project “Solar Collector Continue Façade” (FCCS), funded by the POR FERS Sicilia 2007/2013- Research line 4.1.1.1, two BSTF prototypes were designed and tested. These two BSTF prototypes, depicted in figure 1, are installed into the industrial building of the EUROINFISSI Company, in Ragusa. They are constructed with an aluminum frame specifically designed to be coupled with the solar plate collector type Viessmann Vitosol 200-FM. The designed BSTF may be integrated or, merely overlaid into the façade in case of building renovation.

One of the two BSTF prototype, namely v-BSTF, is mounted leaving a ventilated gap between the FPC and the building envelope.



Fig 16. Map of the building (left side); photo of the two BSTF prototypes (right side)

The ventilated solar thermal façade (v-BSTF) has a total gross surface of 7.50 x 2.40 m and it is constituted by six solar panels, subdivided into two arrays. The v-BSTF is north-west oriented.

The v-BSTF is part of a solar thermal plant, designed for DHW production, equipped with a solar storage tank with a capacity of 1000 liters. The hydronic circuit is managed through a control system that switches on/off the solar pump by controlling the outlet temperature from the solar collector and the temperature in the lowest part of the solar storage tank.

Nearby the pilot v-BSTF, a meteorological station equipped with a set of sensors for the measurements of the outdoor air temperature, global radiation on the vertical plane, wind speed and direction was installed. Moreover, the superficial temperatures on the back of the solar collectors and on the building wall and the air velocity are measured at different heights into the air gap. The air pressure difference between the inlet and outlet sections of the air gap, the superficial temperature on the front of the solar collector and the air temperature in the indoor space were also measured. All the measured parameters were recorded in a data logger[16].

LSI Lastem manufacturer commercializes all the components of the monitoring system. Figure 17 depicts the different sensors installed.






	Outdoor air temperature	Air temperature	Total radiation	Wind speed and direction	Surface temperature
					
Measuring range	-50÷70°C	-50÷70°C	0÷2000W/m <sup>2</sup>	>0.36m/s	-50÷70°C
Accuracy	0.10°C	0.10°C	±5%	1.5%	0.15°C
Response time	30s	30s	23s	0.48s	35s

Figure 17. Features of the main sensors installed

Figure 18 depicts the positions where the sensors were installed on the v-BIST facade and as they are named.

The design of the placement of temperature sensors was conceived for the purpose of evaluated the variation of temperature that is generated by the airflow in the air gap.

The comparison of the temperatures measured with sensor TS7 with the temperatures measured on the building façade ( TS1, TS3, and TS5) allows evaluating the difference of temperature of a surface directly exposed to the sun rays and a shaded surface. Moreover, the lag and fluctuation for the peak temperatures can be evaluated on the above mentioned surfaces.

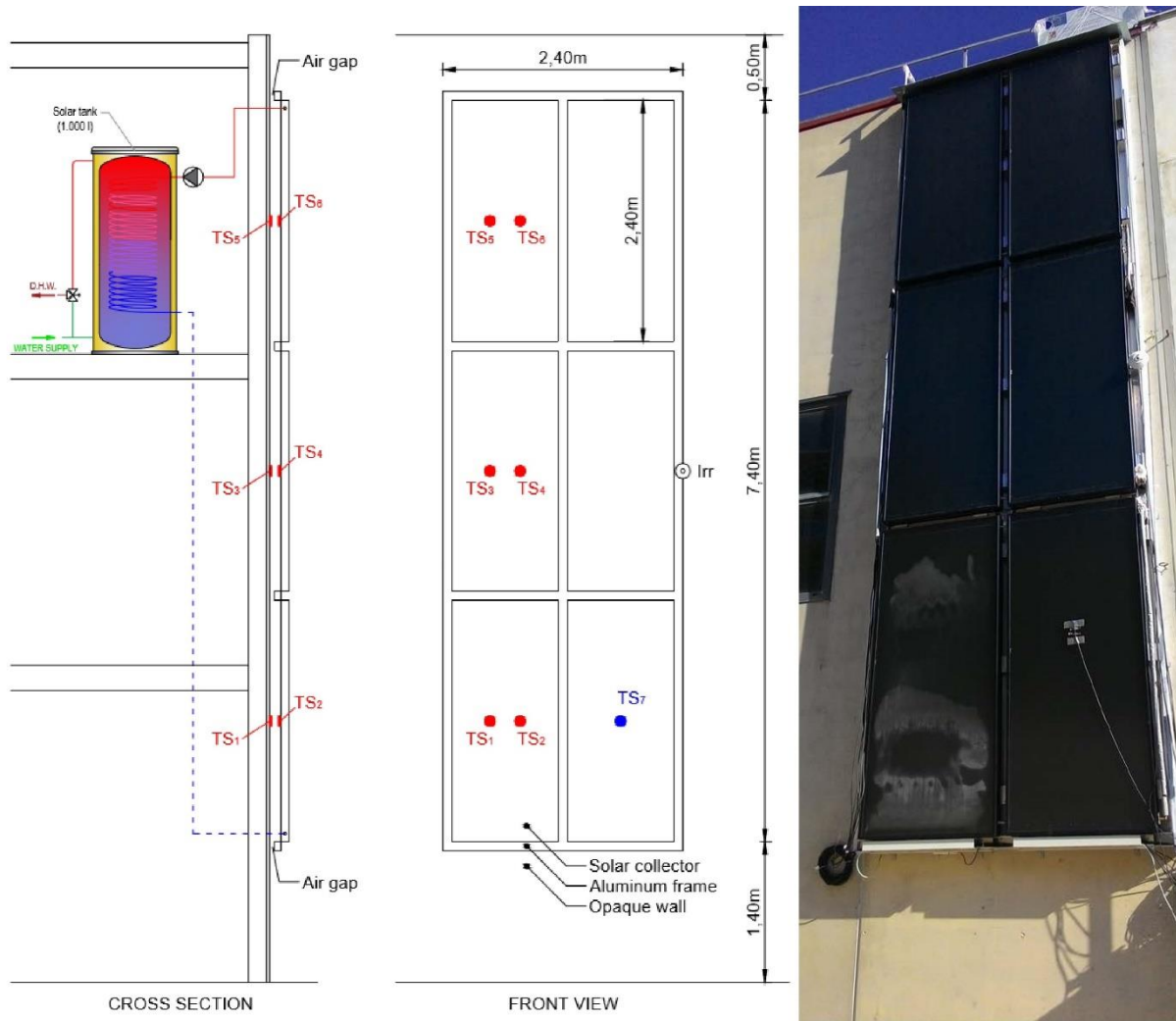


Fig. 18. Section and front view of the v-BSTF façade with the installed sensors

The sensors that measure the surface temperature are called  $T_{S,i}$  ( $i= 1, 2 \dots 7$ ). They are installed in the middle part of each solar panel, three in adherence to the building wall ( $T_{S1}$ ,  $T_{S3}$ , and  $T_{S5}$ ), others three in the back of the solar plate panel ( $T_{S2}$ ,  $T_{S4}$ , and  $T_{S6}$ ). The sensor  $T_{S7}$  is installed into the front face of the lower solar panel of the BSTF.

The comparison of the temperatures measured with sensor  $T_{S7}$  with the temperatures measured on the building façade ( $T_{S1}$ ,  $T_{S3}$ , and  $T_{S5}$ ) allows evaluating the difference of temperature of a surface directly exposed to the sun rays and a shaded surface. Moreover, the time shift between the peaks of temperatures in those surface may be pointed out.

## 6.2 On-Site Measurements

Figure 19 depicts the data collected through the monitoring system during six winter days. The upper part of this figure shows the solar irradiance and the environmental temperature, while in the lower part the temperatures measured by the sensors are depicted.

It is possible to observe that during these sunny days the thermal behavior of the BSTF is quite similar.



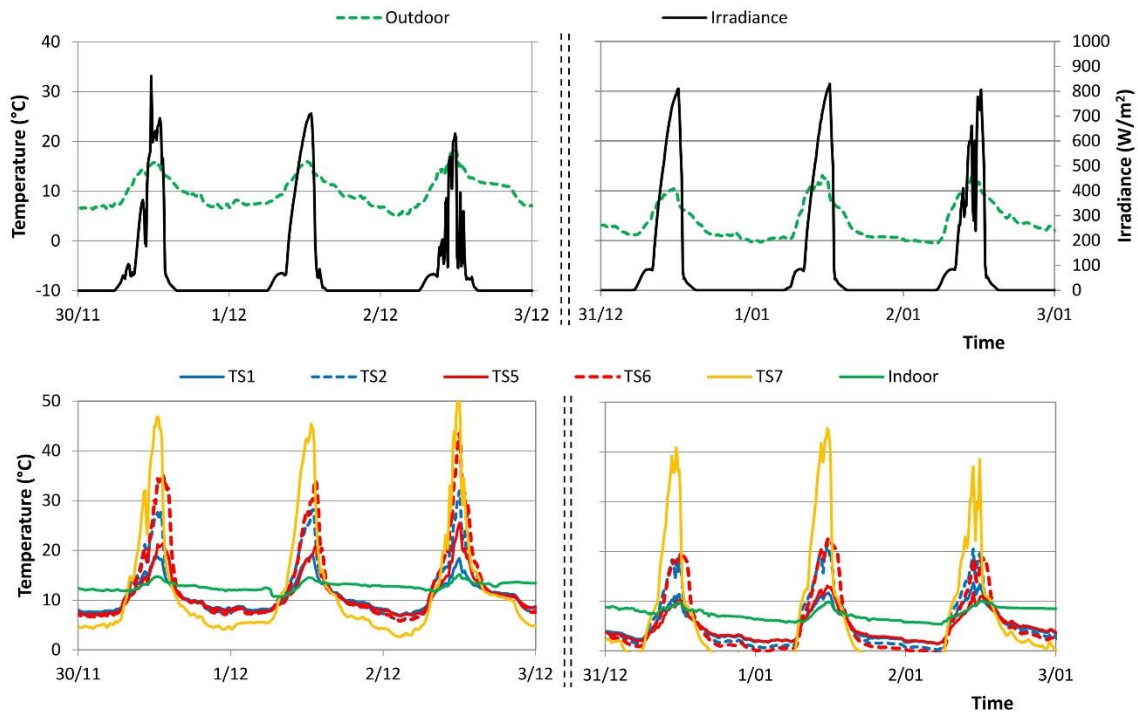


Figure 19. Experimental data of the v-BSTF

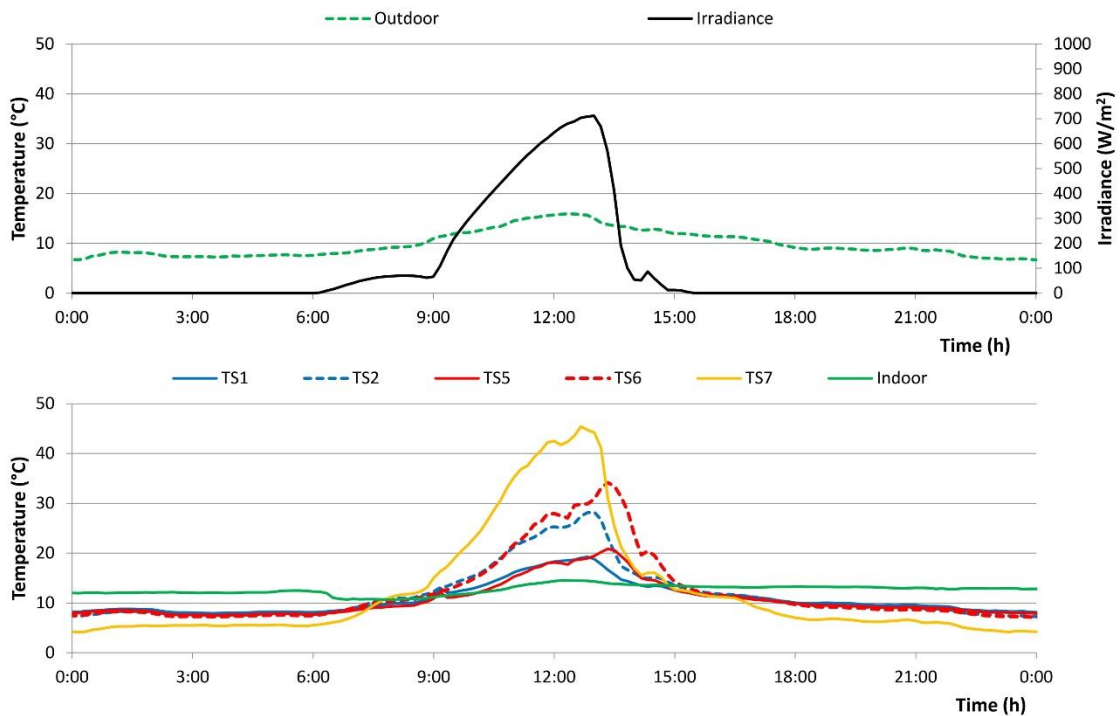


Figure 20 shows the details of the monitored data during one of these days ( 1<sup>st</sup> December)

It is possible to notice that the superficial temperature ( $T_{s7}$ ) on the front of the solar panel is the highest during day-time (the surface is heated by the solar radiation) and it is the lowest during night-time (the surface is cooled by radiative losses versus the skydome). Such temperature has the highest thermal drop.

On the back of the solar collectors, the highest temperature is reached in the upper part of the solar facades ( $T_{s6}$ ).

This means that the surrounding air is heated flowing out in the ventilated air gap. The temperatures differences between the highest and the lowest sensor ( $T_{s6} - T_{s2}$ ) increase during the daytime reaching a maximum of about  $10^{\circ}\text{C}$  about at 13:30.

The temperatures measured on the building facade, ( $T_{s1}$  and  $T_{s5}$ ), once again increase moving from the bottom up of the building façade, reaching a temperature difference of about  $5^{\circ}\text{C}$  ( $T_{s5} - T_{s1}$ ) at 13:30.

During daytime, these temperatures ( $T_{s1}$ , and  $T_{s5}$ ) are permanently higher than the outdoor air temperatures. During night-time a reversal behavior occurs, since the superficial temperatures on the building facade ( $T_{s1}$  and  $T_{s5}$ ) are about  $5^{\circ}\text{C}$  higher than  $T_{s7}$  and close to the outdoor temperature. This result designates a reduction of the radiative heat-losses from the wall surface to the skydome in comparison with a façade directly exposed to the skydome.

Finally, it has to be remarked that the solar façade causes a decrease of the solar gains during the winter period, since a part of the solar energy that strikes the facade is used for heating the fluid in the solar circuit.

However, as well known this shortcoming may be neglected considering that only a low percentage of the solar radiation that strikes the opaque façade is useful for reducing the building thermal load. And also, that during night-time the BSTF allows reducing the heat losses through the building envelope as previously mentioned.

Other interesting beneficial effects arise by the adoption of a BSTF are due to the decrease of the solar gains during the hot season which allows achieving remarkable energy savings, up to 50% [30].

## CONCLUSIONS

This study evaluates the viability of solar thermal plant added to the building facades (BSTF) under different climate conditions. Thus, the energy and environmental analysis of vertical solar thermal facade constructed with flat plate solar collector or evacuated tube solar collector (ETC) used for DHW production have been investigated through numerical simulations by TRNSYS software.

In particular, the performances of the solar façades were investigated in four different Italian cities. The simulations were conducted considering the DHW requirements of a typical Italian family. The results of simulations provide the temperatures reached in the thermal storage, the energy supplied by the solar plant as well as the auxiliary energy supplied.

The comparison among the different cities shows that the BSTF allows reducing the fluctuations of the coverage factor “f” throughout the year, especially when evacuated tube collectors are used. Moreover, during the summer, the reduced solar radiation that hits the vertical surfaces avoids thermal energy overproduction and therefore the risk of overheating and the consequent energy waste.

The yearly analysis highlights that under the scenario 1, BSTF constituted by just  $4.0\text{ m}^2$  of FPC, the coverage factors “f” of about 67% in Catania and Roma, 65% in Ragusa and 44% in Milan are achieved.

Otherwise, under scenario 2, BSTF constituted by just  $4.0\text{ m}^2$  of ETC, an increase of the performance especially in the coldest city (Milan) is obtained. The coverages factors reach values of about 57% in Milan and more than 76% in the other investigated cities.

The proposed simplified economic analysis highlights that the installation of the ETC instead of the FPC involves payback time of about 20 years in Catania, Ragusa and Roma, which does not justify the adoption of the ETC in such cities. In Milan, the payback time is less than 15 years that may be acceptable under the economic point of view instead.

Both the two BSTF have energy and emission payback times less than 2 years, which are very short in comparison with the life cycle of such solar systems.

The high fraction of the DHW energy requirements supplied through the BSTF, as well as the short energy and CO<sub>2</sub> payback times, allow affirming that a vertical solar façade represents a suitable system for DHW production with great environmental conveniences.

### **Acknowledgments.**

This research was developed under the research project Solar Continue Collectors Façade (FCCS) funded by POR FESR Sicilia 2007/2013 - Research line 4.1.1.1. bis.

### **REFERENCES**

- [1] The International Energy Agency IEA, *Key World Energy Statistics 2015*. 2015.
- [2] A. Savvides, C. Vassiliades, A. Michael, and S. Kalogirou, "Siting and building-massing considerations for the urban integration of active solar energy systems," *Renew. Energy*, vol. 135, pp. 963–974, May 2019.
- [3] I. Visa, A. Duta, and M. Moldovan, "Outdoor performance of a trapeze solar thermal collector for facades integration," *Renewable Energy*, 2018.
- [4] S. A. Kalogirou, "Building integration of solar renewable energy systems towards zero or nearly zero energy buildings," *Int. J. Low-Carbon Technol.*, 2015.
- [5] C. Lamnatou, J. D. Mondol, D. Chemisana, and C. Maurer, "Modelling and simulation of Building-Integrated solar thermal systems: Behaviour of the coupled building/system configuration," *Renew. Sustain. Energy Rev.*, 2015.
- [6] A. Buonomano, F. Calise, A. Palombo, and M. Vicidomini, "BIPVT systems for residential applications: An energy and economic analysis for European climates," *Appl. Energy*, 2016.
- [7] H. Gajbert, *Solar thermal energy systems for building integration*. 2008.
- [8] M. C. Munari Probst and C. Roecker, "Towards an improved architectural quality of building integrated solar thermal systems (BIST)," *Sol. Energy*, 2007.
- [9] F. Motte, G. Notton, C. Cristofari, and J. L. Canaletti, "Design and modelling of a new patented thermal solar collector with high building integration," *Appl. Energy*, 2013.
- [10] C. Maurer, C. Cappel, and T. E. Kuhn, "Simple models for building-integrated solar thermal systems," *Energy Build.*, 2015.
- [11] M. V. Albanese, B. S. Robinson, E. G. Brehob, and M. Keith Sharp, "Simulated and experimental performance of a heat pipe assisted solar wall," *Sol. Energy*, 2012.
- [12] A. Buonomano, C. Forzano, S. A. Kalogirou, and A. Palombo, "Building-façade integrated solar thermal collectors: Energy-economic performance and indoor comfort simulation model of a water based prototype for heating, cooling, and DHW production," *Renewable Energy*, 2018.
- [13] M. Beccali, G. Leone, P. Caputo, and S. Ferrari, "Building Integrated Solar Thermal Design: Assessment of Performances of a Low Cost Solar Wall in a Typical Italian Building," in *Energy Procedia*, 2016.
- [14] M. M. Hassan and Y. Beliveau, "Design, construction and performance prediction of integrated solar roof collectors using finite element analysis," *Constr. Build. Mater.*, 2007.
- [15] C. N. Antoniadis and G. Martinopoulos, "Optimization of a building integrated solar thermal system with seasonal storage using TRNSYS," *Renewable Energy*, 2018.
- [16] G. Notton, F. Motte, C. Cristofari, and J. L. Canaletti, "Performances and numerical optimization of a novel thermal solar collector for residential building," *Renewable and Sustainable Energy Reviews*. 2014.
- [17] F. Motte, G. Notton, C. Lamnatou, C. Cristofari, and D. Chemisana, "Numerical study of PCM integration impact on overall performances of a highly building-integrated solar

- collector,” *Renewable Energy*, 2017.
- [18] A. Gagliano, G. M. Tina, F. Nocera, A. D. Grasso, and S. Aneli, “Description and performance analysis of a flexible photovoltaic/thermal (PV/T) solar system,” *Renewable Energy*, 2018.
- [19] T. T. Chow, K. F. Fong, A. L. S. Chan, and Z. Lin, “Potential application of a centralized solar water-heating system for a high-rise residential building in Hong Kong,” *Appl. Energy*, 2006.
- [20] A. Buonomano, G. De Luca, U. Montanaro, and A. Palombo, “Innovative technologies for NZEBs: An energy and economic analysis tool and a case study of a non-residential building for the Mediterranean climate,” *Energy Build.*, 2016.
- [21] S. A. Kalogirou, “Environmental benefits of domestic solar energy systems,” *Energy Convers. Manag.*, 2004.
- [22] F. Ardente, G. Beccali, M. Cellura, and V. Lo Brano, “Life cycle assessment of a solar thermal collector,” *Renew. Energy*, 2005.
- [23] F. Ardente, G. Beccali, M. Cellura, and V. Lo Brano, “Life cycle assessment of a solar thermal collector: Sensitivity analysis, energy and environmental balances,” *Renew. Energy*, 2005.
- [24] C. Lamnatou, G. Notton, D. Chemisana, and C. Cristofari, “Life cycle analysis of a building-integrated solar thermal collector, based on embodied energy and embodied carbon methodologies,” *Energy Build.*, 2014.
- [25] C. Lamnatou, D. Chemisana, R. Mateus, M. G. Almeida, and S. M. Silva, “Review and perspectives on Life Cycle Analysis of solar technologies with emphasis on building-integrated solar thermal systems,” *Renewable Energy*. 2015.
- [26] B. Carlsson, H. Persson, M. Meir, and J. Rekstad, “A total cost perspective on use of polymeric materials in solar collectors - Importance of environmental performance on suitability,” *Appl. Energy*, 2014.
- [27] M. Goedkoop and R. Spriensma, “The Eco-indicator 99 - A damage oriented method for Life Cycle Impact Assessment: methodology report - Third edition,” 2001.
- [28] T. Barker, “Climate Change 2007 Synthesis Report: An Assessment of the Intergovernmental Panel on Climate Change,” 2007.
- [29] S. A. Klein, “TRNSYS 16,” 2006.
- [30] JRC European Commission, “Photovoltaic Geographical Information System (PVGIS),” *Jt. Res. Cent. - Inst. Energy Transp.*, 2017.
- [31] S. A. Kalogirou and Y. Tripanagnostopoulos, “Hybrid PV/T solar systems for domestic hot water and electricity production,” *Energy Convers. Manag.*, 2006.
- [32] R. L. Shrivastava, V. Kumar, and S. P. Untawale, “Modeling and simulation of solar water heater: A TRNSYS perspective,” *Renewable and Sustainable Energy Reviews*. 2017.
- [33] C. K. Leung, C. L. Carmichael, Y. Hayduk, F. Jiang, V. V. Kononov, and A. G. M. Pazdor, “Data mining meets HCI: Data and visual analytics of frequent patterns,” in *Lecture Notes in Computer Science (including subseries Lecture Notes in Artificial Intelligence and Lecture Notes in Bioinformatics)*, 2016.